$$\dot{x} = -\nabla U(x) \cdot A + \eta \qquad (1)$$

In this formula, x, $U(x)$, A and η represent the system state, potential function (system dynamics), bias (an evaluation function indicating the goodness of fit for the system state) and noise (random variation), respectively. This model detects attractors via random walks; the inappropriate system state reduces Value A, and η becomes dominant.

To verify the benefits of this proposed method, attractor selection models were initially used to control and maintain blood flow on continuous flow pumps, comparatively simple systems. Continuous flow VADs mainly consist of a centrifugal pump or an axial flow pump. These pumps can adjust blood flow through changes in rotation speed on the internal impellers. Equation (2) is a general difference equation of formula (1).

$$x(t+1) = x(t) - A(t)\frac{dU(x(t))}{dx(t)} + \eta(t) \qquad (2)$$

To calculate the flow control on continuous flow pumps, the formula symbols were defined as follows: $x(t)$ = a control signal for rotation speed, $U(x)$ = a temporary target function (an approximate potential function with a turning point at $x(t)$ indicating the achievement of objective flow), A = an evaluation function to produce a $U(x)$-turning-point drawing effect, and η = noise. $U(x)$ was set with the Gaussian distribution function, and a parameter for the center of a turning point was defined as c as shown in a formula (3).

$$U(x) = a \times \exp\frac{-(x-c)^2}{2b} + d \qquad (3)$$

Constant a: Amplitude, b:Width of a temporary potential, c: Center of the potential, d: Offset

Value A tends to be high on a true $U(x)$ turning point; therefore, even when accurate $U(x)$ was not obtained because of the difficulty in modeling, c (the center of the $U(x)$ turning point) was updated to the side that had become high in the previous A by increasing or decreasing according to the Value A. This process allowed inaccurate $U(x)$ to draw to a potential neighborhood true value, and adaptive behaviors were expected accordingly. Value A is an important element which influences systems' behaviors. In this trial, we predicted behaviors to gain arbitrary objective blood flow, and experimentally set Formula (4) to provide a high value in case that the current flow is close to the desired value or the current difference from the objective flow is smaller than the previous difference.

$$A(t) = \frac{\exp\left(e \cdot \left(\left|Flow\_r(\tau-1) - Flow(\tau-1)\right| - \left|Flow\_r(\tau) - Flow(\tau)\right|\right)\right)}{\exp\left|f \cdot (Flow\_r(\tau) - Flow(\tau))\right|} \qquad (4)$$

e, f: Constant, $Flow$: Mean flow rate, $Flow\_r$: objective flow rate, τ: observation time of $Flow$

After η was defined as Gaussian noise, a bias was added to the median value according to the increase or decrease in the previous A, in order to improve the search efficiency.

B. Mock Circulation Test

To evaluate behaviors based on the implemented algorithm, control testing on a closed loop for mock circulation was performed using a prototype model of a developing axial flow pump [18]. The axial flow pump used had a structure to rotate the impeller in the brushless direct current motor, and this was the same as a general continuous flow VAD. In addition, the axial flow pump had a mechanism to support the rotor with the internal impeller through fluid dynamic bearing (Figure 1). This pump was connected to a soft reservoir via the inflow and outflow PVC tube (inner diameter: 1/2 in., length: 1 m, respectively), and the supply side on the pump was equipped with the function of circulatory resistance to generate the pump head (Figure 2). The motor of this pump was operated by a widely-used motor driver which was able to change rotation speed via external signals. The working fluid was 37 wt% glycerol-water solution at 27 degrees Celsius.

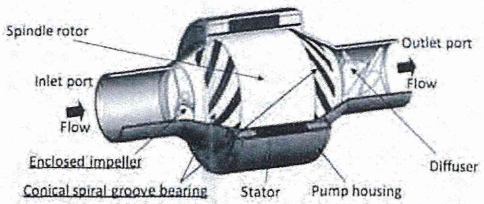

Figure 1. Structural drawing of a prototype axial flow pump under development used in the mock circulation test.

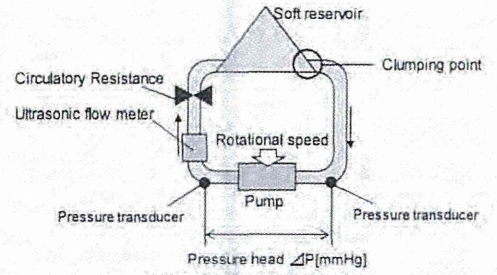

(a) Mock circulation loop

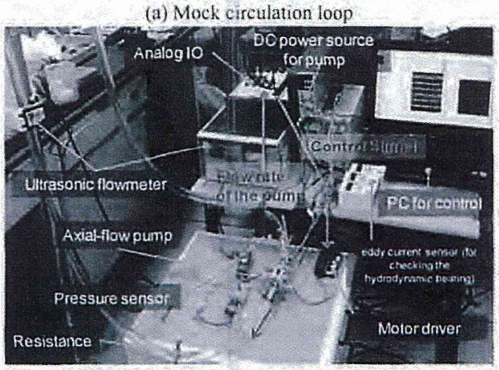

(b) Experimental setup and control system

Figure 2. Schematic diagrams of mock circulation test (measurement items, ⊿P [mmHg]: Pressure sensors, Flow rate [L/min]: Ultrasonic flowmeter, Control signal: x [V], Parameter of the control: $dU(x)$, A, c, n).

The rotation speed control was designed to provide a feedback when any flow signal calculated by the ultrasonic flow meter (T106, Transonic Systems Inc.) is input into the PC and subsequently to output an implementation signal calculated by the proposed algorithm. A pressure sensor (PA-500, Nidec Copal Electronics Corp.) was used to determine the pump inflow- and outflow-side pressure, pump flow measured by the ultrasonic flow meter, and rotation speed control signals and also to record the control parameters ($\Delta U(x)$, A, c, and η). The sampling and parameter updating

cycle were set to 100 Hz and 1 sec, respectively. As the target pump used had a levitated dynamic bearing structure, the algorithm was designed assuming that the actual rotation speed corresponding to rotation speed control signals were known. The rotation speed received from the control signals was set in the range of 7000-12000 rpm so that the bearing was able to maintain stable levitation.

A random rotation number was set to run the pump operation testing. Subsequently, the target flow was set to 5 L/min to begin this control algorithm. Initially, the circulatory resistance was changed to examine the basic behavior, and we observed the variations in the flow, rotation speed, control signal, and other control parameters accordingly. Secondly, inflow sucking (extreme negative pressure on inflow side because of a flow obstruction) was generated on the pump assuming that the environment was unexpectedly changed to evaluate the behavior. The sucking was generated by the tube on the inflow side and the soft reservoir connection part from the outside (Figure 2. (a)), which were unclamped soon after a sucking condition was satisfied (Before this procedure, we conducted a stationary operation to confirm that the negative pressures caused by sucking were not automatically released at the event of full sucking). Similarly, the changes in the pump behaviors were observed.

III. RESULTS

Figure 3 lists the results of the circulatory resistance changes. In this test, our proposed method was used to control the blood flow of an axial flow pump to maintain an arbitrary target flow. The objective flow of 5 L/min was achieved when this control was added to pump operation by the steady rotation speed of 4.5 L/min. Subsequently, when the circulatory resistance was reduced, the following changes were obtained: 1. the pump flow increased, 2. η became

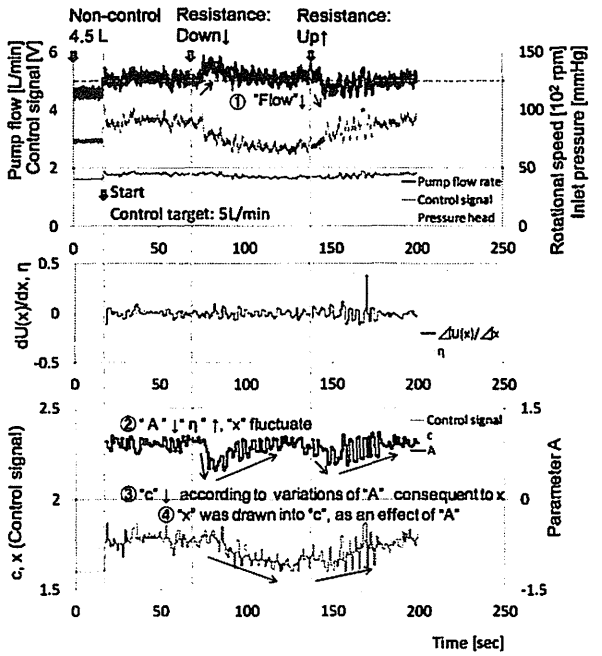

Figure 3. The behavior of the pump to changes of the circulatory resistance

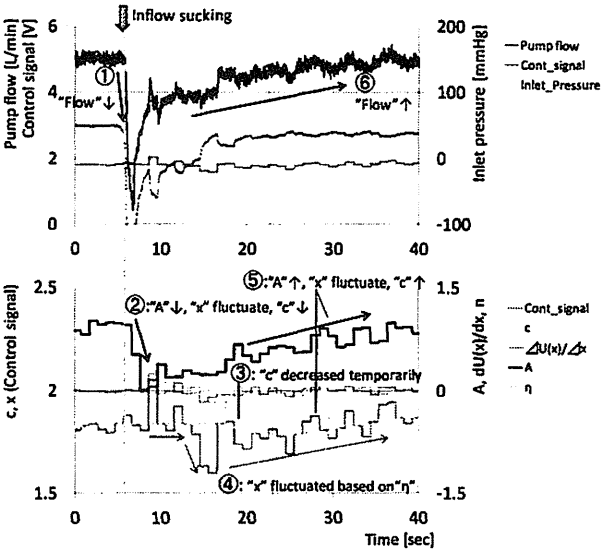

Figure 4. One example of the adaptive behavior on inflow obstruction (unexpected disturbance).

dominant because of a decrease in A and this changed x, 3. c was updated along with the change of A consequent to x, and finally 4. x was drawn into c, the center of $U(x)$, as an effect of A. Accordingly, the flow achieved the desired value again. We observed that the flow achieved to the target value when the circulatory resistance increased further after it had reached the initial value.

Furthermore, one case of behaviors in inflow sucking was listed in Figure 4. According to the result, 1. the flow decreased because of inflow sucking, 2. a decrease in A allowed η to be dominant and this changed A consequent to the variation in x, 3. c temporally decreased, 4. the negative pressure on the inflow side was released after c was drawn into c, 5. A increased because of recovery of the flow and c also increased tentatively, and 6. the flow reached the target value again. Similarly, the target flow was achieved throughout 10-time attempts, even though the results varied widely (24.1±16.4 sec) because of the sucking degrees and noise effects.

IV. DISCUSSION

As tasks of this trial, a rotation speed increase and temporary decrease were required when the blood flow decreased because of a circulatory resistance increase and sucking, respectively. Flow maintenance and sucking release could be realized by other means; however, in this method, different behaviors were required for the same flow-decrease phenomenon. Therefore, the self-adjusting behaviors observed in this study should be significantly useful to develop more flexibly adaptive ventricular assist device control, because those results were obtained without the provision of any additional sensor for sucking detection as well as the design of behavioral rules based on some models or experiences. Furthermore, this study demonstrated that the method was able to cope with dynamic objects and first or low-frequency events regardless of the disadvantages of accuracy and speed. However more detailed behaviors should be investigated for severe conditions on the circulation.

At clinical sites in which continuous flow VADs are used, sucking on the ventricle insert site of an inflow cannula is acknowledged as a problem; thus, this method which can solve sucking automatically is likely useful. In this trial, the probe of the ultrasonic flow meter used was connected to the outflow tube to determine the pump flow. A general continuous flow VAD has a function to estimate flow from current or other values. Nevertheless, it is difficult to provide accurate data in situations such as sucking. Some ultrasonic flow meter probes are able to be used with blood vessel prostheses for VAD blood supply; however, long-term stable measurements of flow are likely difficult in implantable continuous flow VAD patients. As many researchers have pointed out, development of long-term stable flow measurements is a major task with respect to implantable continuous flow VADs [19-22], and this is also essential for this flow control algorithm. Meanwhile, testing under pulsatile pressure must be performed to investigate the behaviors of this algorithm, in consideration of blood inflow from the patient's native heart. With the exception of c, the parameters, constant a, b, d of $U(x)$, control cycle, e & f corresponding to the weight of A, and bias of noise η were set by trial and error approach. To establish the evaluation and design methods to optimize these parameters is another task.

In this trial, the control to maintain flow was executed using the feedbacks of pump flow measurements. This algorithm is able to be applied not only to flow control but also other processes. A and x can be respectively independent in regard to this method. Therefore, if further technical developments enable macroscopic index sensing such as judging on VAD patients' circulation conditions or comfort, pumps using this method may cope with sensing situations easily even if the relationship between the indices of evaluation function A and pump flow is not clear. In addition, combinatory use of this proposed method with currently-used VAD control methods may enable stable VAD systems to behave without algorithm errors, because this method is able to help to adapt other control algorithms to the human body.

V. CONCLUSION

In this study, we proposed a searching control method and performed axial flow pump flow control using a mock circulation loop. As a result, the control to maintain the target flow determined at the design phase was successfully achieved. When sucking, an unexpected event, occurred, the target flow was recovered via the self-adjusting behavior without designing the detailed control rule based on the experience or the model of the control target.

Accordingly, this method was proved useful with respect to autonomous VAD control.

REFERENCES

[1] Slaughter MS, Pagani FD, Rogers JG, *et al.* "Clinical management of continuous-flow left ventricular assist devices in advanced heart failure", J Heart Lung Transplant, 29(45), S1-39, 2010

[2] Garrick C Stewart, Michael M Givertz, "Mechanical circulatory support for advanced heart failure: Patients and technology in evolution", Circulation, 125(10), pp.1304-15, 2012

[3] Kyo S, Minami T, Nishimura T, *et al.* "New era for therapeutic strategy for heart failure: Destination therapy by left ventricular assist device", Journal of Cardiology, 59(2), pp. 101-109, 2012

[4] Sawa Y, "Current status of myocardial regeneration therapy", Gen Thorac Cardiovasc Surg. 2013 Jan;61(1):17-23. doi: 10.1007/s11748-012-0153-9. Epub 2012 Nov 7

[5] AlOmari AH, Savkin AV, Stevens M, Mason DG, Timms DL, Salamonsen RF, Lovell NH, "Developments in control systems for rotary left ventricular assist devices for heart failure patients: a review", Physiol. Meas. 34 R1–R27, 2013

[6] Wu Y, "Adaptive physiological speed/flow control of rotary blood pumps in permanent implantation using intrinsic pump parameters", ASAIO J. , 55(4), pp. 335-9, 2009

[7] Ando M, Nishimura T, Takewa Y, Yamazaki K, Kyo S, Ono M, Tsukiya T, Mizuno T, Taenaka Y, Tatsumi E, "Electrocardiogram-synchronized rotational speed change mode in rotary pumps could improve pulsatility", Artif. Organs, 35(10), pp. 941-947, 2011

[8] Umeki A, Nishimura T, Ando M, Takewa Y, Yamazaki K, Kyo S, Ono M, Tsukiya T, Mizuno T, Taenaka Y, Tatsumi E, "Alteration of LV end-diastolic volume by controlling the power of the continuous-flow LVAD, so it is synchronized with cardiac beat: development of a native heart load control system (NHLCS), J Artif. Organs, 15(2), pp. 128-133, 2012

[9] A. Kashiwagi, I. Urabe, K. Kaneko, T. Yomo, "Adaptive response of a gene network to environmental changes by fitness-induced attractor selection", PLoS ONE, 1: e49, 2006

[10] M. Nishikawa, H. Takagi, T. shibata, A. H. Iwane, T. Yanagida, "Fluctuation Analysis of Mechanochemical Coupling Depending on the Type of Biomolecular Motors", Phys. Rev. Lett. 101, 128103, 2008

[11] M. Iwaki, A. H. Iwane, T. Shimokawa, R. Cooke, T. Yanagida, "Brownian search-and-catch mechanism for myosin-VI steps", Nat. Chem. Biol 5(6), pp. 403-405, 2009

[12] T. Kuusela, T. Shepherd, J. Hietarinta, "Stochastic model for heart-rate fluctuations", Phys Rev E67, 061904, 2003

[13] T. Kuusela, "Stochastic heart-rate model can reveal pathologic cardiac dynamics", Phys Rev E69, 031916, 2004

[14] A. Sugahara, Y. Nakamura, I. Fukuyori, Y. Matsumoto, and H. Ishiguro, Generating circular motion of a human-like robotic arm using attractor selection model. Journal of robotics and mechatronics 22(3), pp. 315-321, 2010

[15] Y. Koizumi, T. Miyamura, S. Arakawa, E. Oki, K. Shiomoto, and M. Murata, Adaptive virtual network topology control based on attractor selection, IEEE/OSA Journal of Lightwave Technology 28(11), pp. 1720-1731, 2010

[16] Y. Minami, Y. Koizumi, S. Arakawa, T. Miyamura, K. Shimoto, M. Murata, "Benefits of Virtual Network Topology Control based on Attractor Selection in WDM Networks", International Journal on Advances in Internet Technology, 4(1- 2), pp. 79-88, 2011

[17] S.G. Nurzaman, Y. Matsumoto, Y. Nakamura, S. Koizumi, and H. Ishiguro, ""Yuragi" based adaptive mobile robot search with and without gradient sensing: from bacterial chemotaxis to Levy walk", Advanced Robotics, 25(16), pp.2019—2037, 2011

[18] Sumikura H, Fukunaga K, Funakubo A, Fukui Y, "Verification of enclosed-impeller for an axial flow blood pump by using computational fluid dynamics analysis", Journal of Life Support Engineering, 20, pp. 9-16, 2008, in japanease

[19] Funakubo A, Ahmed S, Sakuma I and Fukui Y, "Flow rate and pressure head estimation in a centrifugal blood pump", Artif. Organs, 26, pp. 985-990, 2002

[20] Tsukiya T, Taenaka Y, Nishinaka T, *et. al.*, "Application of indirect flow rate measurement using motor driving signals to a centrifugal blood pump with an integrated motor", Artif. Organs, 25, pp. 692-696, 2001

[21] Ogawa D *et. a.l.* , "Indirect flow rate estimation of the NEDO PI Gyro pump for chronic BVAD experiments", ASAIO J. , 52, pp. 266–271, 2006

[22] Kitamura T, Matsushima Y, *et. al.*, "Physical model-based indirect measurements of blood pressure and flow using a centrifugal pump", Artif. Organs, 24, pp. 589-593, 2000

J Artif Organs (2014) 17:135–141
DOI 10.1007/s10047-014-0757-1

ORIGINAL ARTICLE

Artificial Heart (Basic)

Novel control system to prevent right ventricular failure induced by rotary blood pump

Mamoru Arakawa · Takashi Nishimura · Yoshiaki Takewa · Akihide Umeki · Masahiko Ando · Yuichiro Kishimoto · Yutaka Fujii · Shunei Kyo · Hideo Adachi · Eisuke Tatsumi

Received: 5 September 2013 / Accepted: 20 January 2014 / Published online: 7 February 2014

Abstract Right ventricular (RV) failure is a potentially fatal complication after treatment with a left ventricular assist device (LVAD). Ventricular septal shift caused by such devices is an important factor in the progress of RV dysfunction. We developed a control system for a rotary blood pump that can change rotational speed (RS) in synchrony with the cardiac cycle. We postulated that decreasing systolic RS using this system would alter ventricular septal movement and thus prevent RV failure. We implanted the EVAHEART ventricular assist device into seven adult goats weighing 54.1 ± 2.1 kg and induced acute bi-ventricular dysfunction by coronary embolization. Left and RV pressure was monitored, and ventricular septal movement was echocardiographically determined. We evaluated circuit-clamp mode as the control condition, as well as continuous and counter-pulse modes, both with full bypass. As a result, a leftward ventricular septal shift occurred in continuous and counter-pulse modes. The septal shift was corrected as a result of decreased RS during the systolic phase in counter-pulse mode. RV fractional area change improved in counter-pulse (59.0 ± 4.6 %) compared with continuous (44.7 ± 4.0 %) mode. In conclusion, decreased RS delivered during the systolic phase using the counter-pulse mode of our new system holds promise for the clinical correction of ventricular septal shift resulting from a LVAD and might confer a benefit upon RV function.

Keywords Artificial organs · Rotary blood pump · LVAD · Right ventricular failure

M. Arakawa (✉) · Y. Takewa · Y. Kishimoto · Y. Fujii · E. Tatsumi
Department of Artificial Organs, National Cerebral and Cardiovascular Center Research Institute, 5-7-1 Fujishiro-dai, Suita, Osaka 565-8565, Japan
e-mail: a_mamoru@mbn.nifty.com

M. Arakawa · H. Adachi
Department of Cardiovascular Surgery, Saitama Medical Center, Jichi Medical University, Saitama, Japan

T. Nishimura (✉) · S. Kyo
Department of Cardiac Surgery, Tokyo Metropolitan Geriatric Hospital, 35-2 Sakae-cho, Itabashi-ku, Tokyo, 173-0015, Japan
e-mail: takashin-tyk@umin.ac.jp

T. Nishimura · A. Umeki · M. Ando
Department of Cardiothoracic Surgery, University of Tokyo, Tokyo, Japan

Introduction

Left ventricular assist device (LVAD) therapy is considered effective for treating patients with end-stage heart failure, either as a bridge to transplantation [1] or as destination therapy [2]. Continuous-flow LVADs are now widely applied, owing to a decrease in complications and improved prognoses compared with pulsatile LVADs [3]. However, differences in physiological effects between continuous-flow and pulsatile LVADs remain controversial [4–6], especially those involving right ventricular (RV) function [7]. The probability of RV failure does not seem to differ between pulsatile and continuous-flow LVADs [7], but differences in the physiological effects between these devices remain unclear.

RV failure is a life-threatening complication for patients treated with an LVAD [8]. Physiologically, an LVAD is thought to have both beneficial and adverse effects on the right ventricle [9, 10]. One reason for the beneficial effect on RV function is that LVAD unloading leads to a decrease in RV afterload through a decrease in pulmonary artery

pressure [11]. However, some reports have indicated that a change in left ventricular (LV) geometry, especially that resulting from a ventricular septal (VS) shift, leads to decreased RV contractility [11, 12]. A VS shift occurs during treatment with LVADs, especially under full or excess LVAD support [10]. Patients with an LVAD who develop RV failure often have concurrent multiple organ failure [13], for which they require high blood-flow support. Therefore, we often encounter the dilemma that increased RS causes RV dysfunction and consequently decreases systemic blood flow. Ultimately, we implant an RV assist device if a patient does not respond to medical therapy [8]. Ideally, an LVAD should provide not only maximum flow support but also RV functional support.

We consider that a change during the LVAD support phase can control RV function, especially that of the ventricular septum. Hence, we developed a novel heart beat-synchronous drive mode for the EVAHEART centrifugal LVAD (Sun Medical Technology Research Corporation, Nagano, Japan) [14]. To create this drive mode, we defined the duration and rotational speed (RS) of the systolic and diastolic phases to drive the EVAHEART in synchrony with the native cardiac cycle [15–18]. This driving mode, which is synchronous with the heartbeat, significantly changes coronary flow in normal goats [16, 17]. We speculated that a VS shift under continuous-flow LVAD support would occur during the complete cardiac cycle. However, VS function is more essential in the systolic than the diastolic phase and this novel drive mode might confer a benefit on VS and RV function under full bypass conditions by decreasing RS during the systolic phase.

We investigated whether the new drive mode could prevent RV failure in a goat model of bi-ventricular dysfunction and evaluated interaction between the left and right ventricles, including VS movement.

Materials and methods

Animals

Seven adult goats weighing 54.1 ± 2.1 kg were maintained in accordance with the guidelines of the Committee on Animal Studies at the National Cerebral and Cardiovascular Center, and the National Cerebral and Cardiovascular Center Animal Investigation Committee approved the study.

Surgical procedures and implanted devices

All animals were sedated with an intramuscular injection of ketamine hydrochloride (8–10 mg/kg) and anesthetized using isoflurane (1–3 vol %/100 mL in oxygen) inhalation. The animals were placed in the right recumbent position, intubated and mechanically ventilated. We approached the pressure lines for aortic and central venous pressure via a left thoracotomy at the fifth intercostal space from the left intrathoracic artery and vein, respectively. The main pulmonary artery and ascending aorta were dissected and taped, and we attached EMF-1000 electromagnetic flow meters (Nihon Kohden, Tokyo, Japan) with a 12–18-mm diameter to them. After heparinization (300 U/kg), the EVAHEART (Sun Medical Technology Research Corporation, Nagano, Japan) was installed without a cardiopulmonary bypass. First, we sutured the outflow conduit of the device to the descending aorta using a partial clamp. Then we made stitches around the LV apex and punched out the apex with a 16-mm puncher. The inflow cannula was immediately inserted using left hand to control bleeding by squeezing as necessary. We used a 16-mm TS420 ultrasonic flow meter (Transonic Systems, Ithaca, NY, USA) to measure LVAD flow (PF). Total flow (TF) was calculated as the sum of the ascending aortic flow and the PF. The bypass rate was calculated by dividing the PF by the TF.

To obtain pressure–volume loops, we inserted a 6-Fr conductance catheter (2S-RH-6DA-116; Taisho Biomed Instruments Co., Ltd., Osaka, Japan) into the RV from the apex towards the pulmonary valve, and 4-Fr micro-tip catheter pressure transducers (Millar Instruments Inc., Houston, TX, USA) were inserted through the RV and LV walls. In addition, pulmonary artery pressure was monitored via a catheter inserted directly into the artery. Hemodynamic data were recorded using LabChart 7 software (ADInstruments, Castle Hill, New South Wales, Australia). The pressure and volume data of the LV were recorded using a Leycom Sigma 5 system (CardioDynamics, Zoetermeer, The Netherlands). We defined LV and RV systolic duration (%) as the sum of the isovolemic contraction phase and the ejection phase of the respective ventricles divided by the RR interval (Fig. 2). Because blood was ejected during the diastolic phase under LVAD support, we defined the end of ejection phase as the first point when RV volume reached diastolic volume and the first point when the ventricular pressure waveform sharply decreased (Fig. 2). The corresponding systolic duration was measured using LabChart software.

Bi-ventricular dysfunction model

We modeled bi-ventricular dysfunction in this study. We impaired RV and LV function by embolizing the coronary artery through the left anterior descending (LAD) and right coronary (RCA) arteries as described [18]. Briefly, a 4-Fr Amplatz catheter (Create Medic Co., Ltd., Yokohama, Japan) was inserted through a 4-Fr long sheath into the left

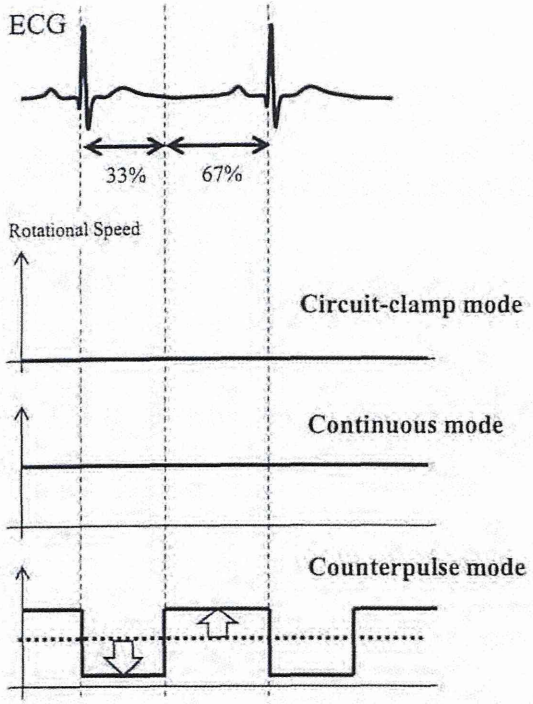

Fig. 1 Rotary blood-pump control modes. Circuit-clamp mode (control) does not include pump support because left ventricular assist device circuit is clamped. Rotational speed in continuous mode remains constant without a controller and that during systolic phase in counter-pulse mode is decreased by a controller. Systolic and diastolic phases in cardiac cycle are defined as 33 and 67 %, respectively, of RR interval

carotid artery toward the LAD and RCA ostia under fluoroscopic guidance. Microspheres (75-μm diameter) were injected into the LAD (60 spheres/kg) and RCA (30 spheres/kg). The general condition of each goat was observed for a further 30 min to stabilize cardiac function before collecting data.

We controlled the infusion volume and depth of anesthesia during the experiment to maintain stable PF and aortic and central venous pressures, thus avoiding suction at the inflow cannula and sustaining an appropriate after load. All animals were administered with lidocaine 2 % (1 mg/kg/h) during the experiment to prevent ventricular arrhythmia. Heart failure was established to reduce and then maintain cardiac output at approximately 60 % of the cardiac output as TF and PAF according to previously described methods [18].

Study protocol and LVAD control

Our new controller allows the RS of the EVAHEART to change for a specific duration after an R wave appears to synchronize it with the cardiac cycle. We defined the systolic and diastolic phases of the cardiac cycle as 33 and 67 % of the RR interval, respectively, (Fig. 1) according to the published protocol [15–18]. The pressure and flow parameters described above were evaluated twice in each goat under the following LVAD controller modes (Fig. 1): circuit-clamp (no pump support due to clamping the LVAD circuit) as the control condition, continuous (constant RS without using the new controller) and counter-pulse (RS decreased during systolic phase using the new controller). We set the RS during the systolic phase to 700–1,000 rpm in the counter-pulse mode and increased the RS in the diastolic phase to achieve an appropriate bypass rate, which was calculated by dividing the PF rate by the sum of the flow rates of the PF and the ascending aorta. We defined full bypass as a rate of about 100 % (range 90–110 %).

Echocardiography

We evaluated RV and LV dimensions by echocardiography using a Vivid E9 system and M5S-D sector transducer (GE Healthcare, Horten, Norway). The end-diastolic and end-systolic RV areas were measured in the direct cardiac long-axis view. The %fractional area change was calculated as:

$$\frac{\text{end - diastolic RV area} - \text{end - systolic RV area}}{\text{end - diastolic RV area}} \times 100$$

Statistical analysis

Numerical data are shown as mean ± SE. Differences in values between groups were analyzed by repeated measures analysis of variance followed by Tukey's multiple comparison test. Statistical significance was accepted at a probability value of <0.05. All data were analyzed using SPSS version 19 (SPSS Inc., Chicago, IL, USA).

Results

Bi-ventricular dysfunction models were established by coronary embolism in which TF decreased from 3.3 ± 0.4 to 2.0 ± 0.3 L/min ($p < 0.01$) in the circuit-clamp mode. The dP/dt, particularly in the RV, fell from 436 ± 40 to 341 ± 48 mmHg/s ($p < 0.05$) and E_{max} fell from 1.35 ± 0.16 to 0.87 ± 0.19 ($p < 0.05$) in circuit-clamp mode.

Figure 2 shows sample waveforms of the ECG, R waves, RV pressure, LV pressure, PF, and RS. Actual RS in the counter-pulse mode closely followed the command RS, since average RS in the systolic and the diastolic phase was close. LV pressure waveforms were decreased in the continuous mode. The amplitude of the LV pressure waveforms was similar between counter-pulse and circuit-clamp modes. The duration of the systolic phase differed among the three groups (Fig. 3). The duration of systole

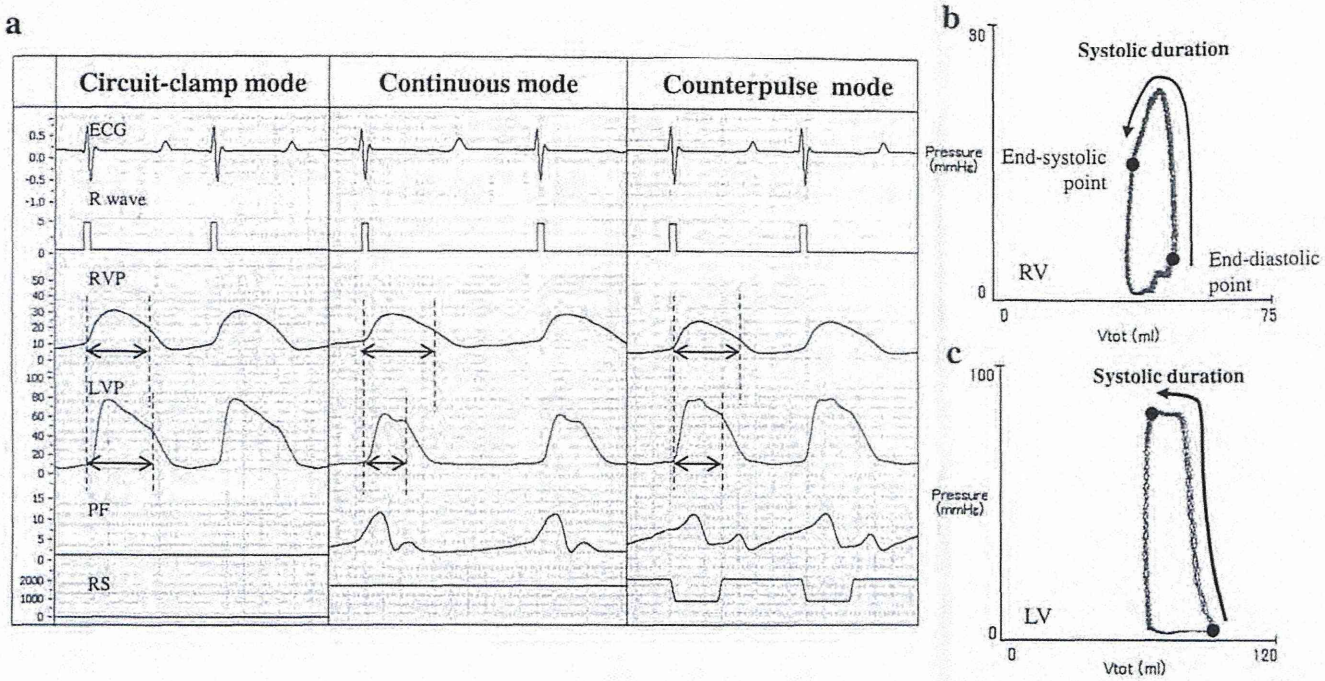

Fig. 2 Sample pressure and flow waveforms and pressure–volume loops for each mode. **a** Left ventricular systolic duration is decreased in continuous mode compared with that in circuit-clamp mode. Duration of LV systolic phase is longer in counter-pulse than in continuous mode. *LV* left ventricular pressure, *PF* pump flow, *RS* rotational speed, *RVP* right ventricular pressure. **b**, **c** Left and right ventricular systolic duration (%) is the sum of isovolumic contraction and ejection phases of respective ventricles divided by cardiac cycle

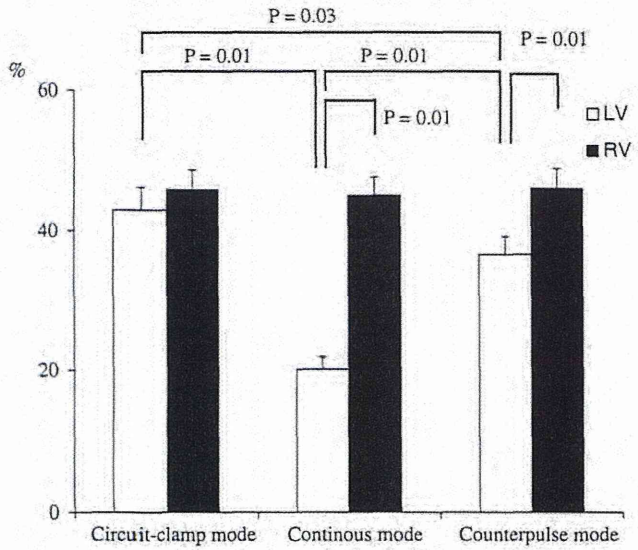

Fig. 3 Systolic duration per mode. Left ventricular systolic phase is significantly shorter than RV systolic phase in continuous mode, and shorter than LV systolic phase in circuit-clamp mode. Left ventricular systolic phase is significantly shorter in counter-pulse than in circuit-clamp mode, and longer than in continuous mode. *LV* left ventricle, *RV* right ventricle

between the right and left ventricles did not significantly differ in circuit-clamp mode (45.8 ± 2.8 vs. 42.9 ± 3.2 %, respectively). The LV systolic phase was significantly shorter than the RV systolic phase in the continuous mode and the LV systolic phase in circuit-clamp mode (LV vs. RV: 20.2 ± 1.8 vs. 45.0 ± 2.5 %, $p = 0.01$). The LV systolic phase was significantly shorter in the counter-pulse, than in the circuit-clamp mode, and significantly longer than in the continuous mode (RV 45.9 ± 2.7 vs. LV 36.5 ± 2.6 %; $p = 0.01$) (Fig. 3).

Table 1 shows the LV and RV data. The LV end-diastolic pressure was significantly decreased in LVAD modes (continuous and counter-pulse modes) compared with circuit-clamp mode. The RV end-diastolic pressure and volume did not significantly differ among the three modes. In addition, pulmonary artery pressure slightly decreased and pulmonary artery flow was slightly higher during the LVAD modes than in circuit-clamp mode, although mean RS in the counter-pulse mode was significantly lower than that of the continuous mode.

RV free wall movement did not significantly change in counter-pulse mode, but VS movement differed among the groups in the direct cardiac short- and long-axis views (Fig. 4). The VS shifted towards the left ventricle in LVAD modes. However, the VS shift was corrected as a result of RS being decreased during the systolic phase in the counter-pulse mode. The end-diastolic RV areas were greater in the LVAD than in circuit-clamp mode. Therefore, the %fractional area change was greater in counter-

Table 1 Hemodynamic data obtained in each drive mode

	Mode		
	Circuit-clamp	Continuous	Counter-pulse
LV			
LVEDP (mmHg)	8.8 ± 1.7	4.7 ± 1.4	4.4 ± 1.2
Mean AoP (mmHg)	59.7 ± 3.0	64.0 ± 3.8	66.0 ± 4.6
Pump flow (L/min)	0.0 ± 0.0	2.4 ± 0.2[a]	2.4 ± 0.2[b]
Total flow (L/min)	2.0 ± 0.3	2.3 ± 0.3	2.3 ± 0.3
Bypass rate (%)	0.0 ± 0.0	107.5 ± 2.4[a]	101.8 ± 3.7[b]
RV			
RVEDP (mmHg)	8.4 ± 1.8	7.9 ± 1.8	8.0 ± 2.0
RVEDV (ml)	75.1 ± 7.8	75.0 ± 8.1	77.8 ± 7.5
d*P*/d*t* max (mmHg/s)	341 ± 48	361 ± 54	381 ± 57
E_{max}	0.87 ± 0.19	0.93 ± 0.22	1.05 ± 0.20
PVA (mmHg/mL)	474 ± 50	522 ± 61	519 ± 50
Mean PAP (mmHg)	27.6 ± 1.9	26.2 ± 0.9	25.4 ± 1.9
PA flow (L/min)	2.1 ± 0.3	2.3 ± 0.3	2.4 ± 0.3
RS			
Actual RS (command RS)			
Systolic RS (rpm)	0 ± 0	1557 ± 53[a] (1588 ± 38[a])	700 ± 23[b,c] (719 ± 12[b,c])
Diastolic RS (rpm)	0 ± 0	1557 ± 53[a] (1588 ± 38[a])	1627 ± 65[b] (1612 ± 46[b,c])
Mean RS (rpm)	0 ± 0	1557 ± 53[a] (1588 ± 38[a])	1290 ± 50[b,c] (1292 ± 36[b,c])

AoP arterial pressure, *LVEDP* left ventricular end-diastolic pressure, *PA* pulmonary artery, *PAP* pulmonary artery pressure, *PVA* pressure volume area, *RS* rotational speed, *RVEDP* right ventricular end-diastolic pressure, *RVEDV* right ventricular end-diastolic volume

[a] $p < 0.01$: circuit-clamp vs. continuous mode

[b] $p < 0.01$: circuit-clamp vs. counter-pulse mode

[c] $p < 0.01$: continuous vs. counter-pulse mode

pulse than in circuit-clamp and continuous modes (59.0 ± 4.6 vs. 56.1 ± 8.8 and 44.7 ± 4.0 %; Fig. 5).

Discussion

To our knowledge, this is the first echocardiographic demonstration of a VS shift being corrected towards the left ventricle in the systolic phase using counter-pulse mode applied to an LVAD. The shift itself might exacerbate RV dysfunction. We consider that LVAD unloading was a major cause of the VS shift, since the duration of the systolic phase was remarkably reduced in continuous mode. The decreased systolic RS provided by the counter-pulse mode significantly corrected LV systolic duration and RV %fractional area change compared with continuous mode. We found that the shortened systolic duration in the continuous mode was corrected in the counter-pulse mode as re-synchronization between the RV and the LV. Thus, we presumed that this favorable effect on RV function was caused by re-synchronizing RV and LV contractions.

Others have discussed the question of whether or not RV function is diminished in patients treated with an LVAD [9–11], especially of the continuous-flow type [7]. We did not find adverse effects on any parameter of RV contractility, such as E_{max}, d*P*/d*t* and pulmonary artery flow. Umeki et al. have demonstrated that the same counter-pulse mode decreases LV end-diastolic volume (LVEDV). They argued the decreased LVEDV and LVEDP directed the unloading effect according to the Staring law. In addition, lower LVEDP decreased RV afterload. However, improvements in RV contractility, such as increased E_{max} or RV diastolic volume, were not evident in counter-pulse compared with continuous mode, although pulmonary flow was slightly increased. In contrast, we confirmed by echocardiography that the novel counter-pulse mode used with the EVAHEART corrected the VS shift during the systolic phase while maintaining a full bypass without a decrease in total systemic flow or adversely affecting the RV. We considered that the counter-pulse mode did not improve RV function because this experiment proceeded under open-chest conditions. That is to say, this mode did not affect the ventricular free wall, which in the right ventricle is important for RV pressure and volume. Taken together, this mode might confer benefits on the right ventricle through the ventricular septum. Park et al. showed that RV performance was impaired by full assist of a left heart bypass with continuous-flow LVAD [10]. Yoshioka et al. [13] discovered that patients with an LVAD who develop RV failure often had concurrent multiple organ failure, for which they required high blood-flow support. We often encounter the dilemma that full LV support causes RV dysfunction and consequently decreases systemic blood flow. Ultimately, some patients required RV assist devices if they did not respond to medical therapy [8]. Our counter-pulse mode can provide not only maximum flow support but also optimized VS movement by only LVADs. We believe that the counter-pulse mode can resolve these issues.

Electrocardiography-synchronized RS control confers several advantages on hemodynamics as well as native heart function compared with continuous RS. Ando et al. [16] created pulsatility using their pulsatile mode with increased RS. Kishimoto et al. [19] reported that speed modulation fully opens the aortic valve and thus prevents aortic insufficiency. Electrocardiography-synchronized RS control of the rotary blood pump confers several beneficial effects compared with the conventional constant RS drive mode. Here, we demonstrated that the system has potential

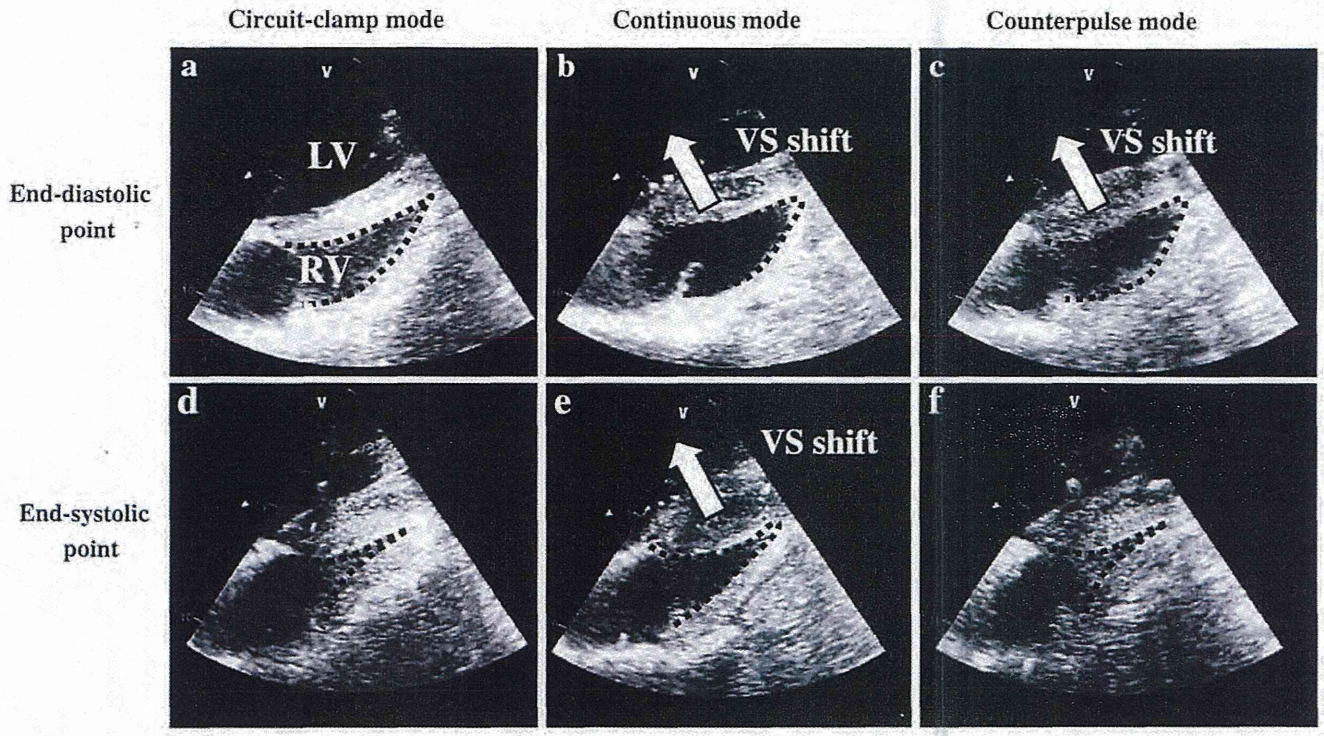

Fig. 4 Sample echocardiograms obtained in each mode. Leftward ventricular septal (VS) shift is evident in continuous and counter-pulse modes (**a**, **b**, **d**, **e**), but corrected by decreased rotational speed during systolic phase in counter-pulse mode (**c**, **f**)

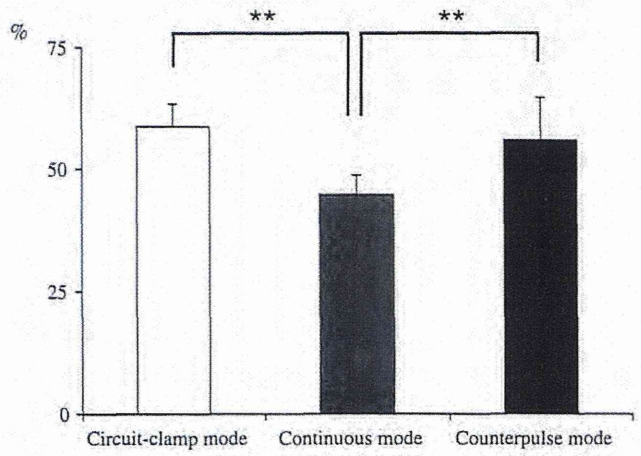

Fig. 5 Bar graph shows right ventricular fractional area change with each mode, $^{**}p < 0.01$

RV support by VS shift correction in addition to the advantages described above. RS control provides further treatment options for circulatory support therapy with rotary blood pumps.

Our study had several limitations. We used an animal model of bi-ventricular dysfunction that developed decreased contractility including that of the ventricular septum. Although VS movement could be evaluated in this model, we could not assess the septal thinning that is a frequent feature of patients with an enlarged LV treated with an LVAD. The next step will be to evaluate VS shift using the new control system in a model with a thin ventricular septum. The experiments proceeded under open-chest condition under which, RV pressure might be difficult to evaluate, since RV pressure remarkably changed according to pressure in the pericardial space. Therefore, the effect of the novel control system should be assessed in a model of chronic heart failure with a thinned ventricular septum under closed-chest conditions.

Conclusion

The novel counter-pulse mode optimized LV unloading and thus corrected VS movement while maintaining sufficient blood flow. This might prevent the RV failure that frequently complicates patients treated with an LVAD, especially during the unstable acute phase after LVAD implantation.

Acknowledgments This study was presented at the annual conference of The American Society for Artificial Internal Organs in 2012, in San Francisco, CA and supported by a JSAO Grant in 2013. The authors are grateful to Dr. Daisuke Ogawa at the Sun Medical Technology Research Corporation for creating the programs.

Conflict of interest The authors have no conflicts of interest to disclose.

References

1. Miller LW, Pagani FD, Russell SD, John R, Boyle AJ, Aaronson KD, Conte JV, Naka Y, Mancini D, Delgado RM, MacGillivray TE, Farrar DJ, Frazier OH, HeartMate II, Clinical investigators. Use of a continuous-flow device in patients awaiting heart transplantation. N Engl J Med. 2007;357:885–96.
2. Lietz K, Long JW, Kfoury AG, Slaughter MS, Silver MA, Milano CA, Rogers JG, Naka Y, Mancini D, Miller LW. Outcomes of left ventricular assist device implantation as destination therapy in the post-REMATCH era: implications for patient selection. Circulation. 2007;116:497–505.
3. Slaughter MS, Rogers JG, Milano CA, Russell SD, Conte JV, Feldman D, Sun B, Tatooles AJ, Delgado RM 3rd, Long JW, Wozniak TC, Ghumman W, Farrar DJ, Frazier OH, HeartMate II Investigators. Advanced heart failure treated with continuous-flow left ventricular assist device. N Engl J Med. 2009;361:2241–51.
4. Garatti A, Bruschi G, Colombo T, Russo C, Lanfranconi M, Milazzo F, Frigerio M, Vitali E. Clinical outcome and bridge to transplant rate of left ventricular assist device recipient patients: comparison between continuous-flow and pulsatile-flow devices. Eur J Cardio Thorac Surg. 2008;34:275–80.
5. Koenig SC, Pantalos GM, Gillars KJ, Ewert DL, Litwak KN, Etoch SW. Hemodynamic and pressure-volume responses to continuous and pulsatile ventricular assist in an adult mock circulation. ASAIO J. 2004;50:15–24.
6. Nishinaka T, Tatsumi E, Nishimura T, Taenaka Y, Masuzawa T, Nakata M, Takano H, Koyanagi H. Cardiac autonomic nervous function during long-term nonpulsatile left heart bypass. Artif Organs. 1999;23:500–3.
7. Patel ND, Weiss ES, Schaffer J, Ullrich SL, Rivard DC, Shah AS, Russell SD, Conte JV. Right heart dysfunction after left ventricular assist device implantation: a comparison of the pulsatile HeartMate I and axial-flow HeartMate II devices. Ann Thorac Surg. 2008;86:832–40.
8. Baumwol J, Macdonald PS, Keogh AM, Kotlyar E, Spratt P, Jansz P, Hayward CS. Right heart failure and "failure to thrive" after left ventricular assist device: clinical predictors and outcomes. J Heart Lung Transplant. 2011;30:888–95.
9. Omoto T, Tanabe H, LaRia PJ, Guererro J, Vlahakes GJ. Right ventricular performance during left ventricular unloading conditions: the contribution of the right ventricular free wall. Thorac Cardiovasc Surg. 2002;50:16–20.
10. Park CH, Nishimura K, Kitano M, Okamoto Y, Ban T. Right ventricular performance is impaired by full assist of left heart bypass. Analysis of right ventricular performance against change in afterload in heart failure models. ASAIO J. 1994;40:M303–8.
11. Kitano M, Nishimura K, Hee PC, Okamoto Y, Ban T. Right ventricular function evaluated by volumetric analysis during left heart bypass in a canine model of postischemic cardiac dysfunction. J Thorac Cardiovasc Surg. 1995;109:796–803.
12. Daly RC, Chandrasekaran K, Cavarocchi NC, Tajik AJ, Schaff HV. Ischemia of the interventricular septum. A mechanism of right ventricular failure during mechanical left ventricular assist. J Thorac Cardiovasc Surg. 1992;103:1186–91.
13. Yoshioka D, Sakaguchi T, Saito S, Miyagawa S, Nishi H, Yoshikawa Y, Fukushima S, Saito T, Daimon T, Ueno T, Kuratani T, Sawa Y. Predictor of early mortality for severe heart failure patients with left ventricular assist device implantation: significance of INTERMACS level and renal function. Circ J. 2012;76:1631–8.
14. Yamazaki K, Kihara S, Akimoto T, Tagusari O, Kawai A, Umezu M, Tomioka J, Kormos RL, Griffith BP, Kurosawa H. EVA-HEART: an implantable centrifugal blood pump for long-term circulatory support. Jpn J Thorac Cardiovasc Surg. 2002;50:461–5.
15. Ando M, Nishimura T, Takewa Y, Ogawa D, Yamazaki K, Kashiwa K, Kyo S, Ono M, Taenaka Y, Tatsumi E. A novel counterpulse drive mode of continuous-flow left ventricular assist devices can minimize intracircuit backward flow during pump weaning. J Artif Organs. 2011;14:74–9.
16. Ando M, Nishimura T, Takewa Y, et al. Electrocardiogram-synchronized rotational speed change mode in rotary pumps could improve pulsatility. Artif Organs. 2011;35:941–7.
17. Ando M, Takewa Y, Nishimura T, Yamazaki K, Kyo S, Ono M, Tsukiya T, Mizuno T, Taenaka Y, Tatsumi E. A novel counterpulsation mode of rotary left ventricular assist devices can enhance myocardial perfusion. J Artif Organs. 2011;14:185–91.
18. Umeki A, Nishimura T, Ando M, Takewa Y, Yamazaki K, Kyo S, Ono M, Tsukiya T, Mizuno T, Taenaka Y, Tatsumi E. Alteration of LV end-diastolic volume by controlling the power of the continuous-flow LVAD, so it is synchronized with cardiac beat: development of a native heart load control system (NHLCS). J Artif Organs. 2012;15:128–33.
19. Kishimoto Y, Takewa Y, Arakawa M, Umeki A, Ando M, Nishimura T, Fujii Y, Mizuno T, Nishimura M, Tatsumi E. Development of a novel drive mode to prevent aortic insufficiency during continuous-flow LVAD support by synchronizing rotational speed with heartbeat. J Artif Organs. 2013;16:129–37.